Quantitative Evaluation of Active Fire Detection Capabilities from VIIRS

Ivan Csiszar[1], Wilfrid Schroeder[2], Evan Ellicott[2] Louis Giglio[2] and Christopher O. Justice[2]

[1] NOAA/NESDIS Center for Satellite Applications and Research, Camp Springs, MD (ivan.csiszar@noaa.gov) [2] University of Maryland - College Park, MD

INTRODUCTION

The VIIRS (Visible/Infrared/Imager/Radiometer Suite) instrument on board the JPSS (Joint Polar Satellite System) and the NPOESS Preparatory Project (NPP) satellites will provide radiometric measurements that offer useful information for the detection of active fires. The baseline algorithm for the VIIRS Active Fire Mask Application Related Product (ARP) uses primarily the medium resolution M13 (4.05 µm) and M15 (10.76 µm) measurements, aggregated from the native resolution observations into medium resolution pixels according to a scheme aimed at reducing the decrease of resolution towards the edges of the scanline. In this work we analyzed the fire detection and characterization potential of the VIIRS sensors, including 1. the use of native spatial resolution radiometric measurements, which would potentially enable earlier detection of fires to support fire early warning, monitoring and management; and 2. the expected saturation of M15, which potentially impacts characterization of a range of fires. For the analysis we developed a modeling framework using a set of coincident fire observations by the ASTER (Advanced Spaceborne Thermal Emission and Reflection Radiometer) and MODIS (Moderate Resolution Imaging Spectroradiometer) sensors on the NASA Earth Observing System Terra satellite, as well as statistical relationships between VIIRS and Aqua/MODIS radiances via direct simulations. The cases analyzed include a wide range of fire characteristics, and environmental and observing conditions.

SIMULATION OF VIIRS FIRE PIXEL RADIANCES

MODIS can be considered as the precursor instrument to VIIRS, providing similar radiometric measurements for fire observations at 1km nadir resolution for the mid-IR and IR bands. The principal issue of using MODIS as a proxy for VIIRS for fire pixels is the need to account for the variation of the sub-pixel area of active burning and the resulting differences between the integrated radiometric signals over the MODIS and VIIRS pixel footprints. This is particularly important when simulating VIIRS radiances in the presence of fires at native resolution.

ASTER input data are used to generate VIIRS middle and thermal infrared proxy data. VIIRS spectral and spatial characteristics are accounted for during proxy data generation. Atmospheric and solar components are simulated using MODTRAN radiative transfer code based on input radiosonde or model data.

Thermal Infrared Data

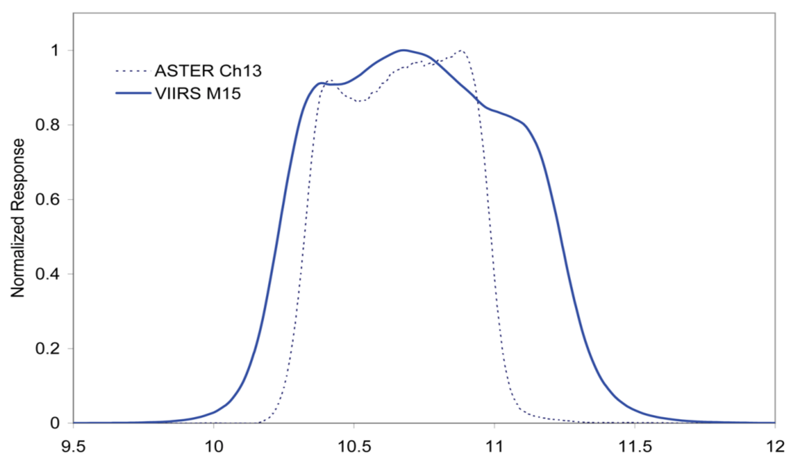

ASTER channel 13 is used to approximate VIIRS channel M15; the spectral response functions of the two channels are comparable therefore no additional spectral transformation is performed.

Spectral response curves for 90m ASTER channel 13 and 750m VIIRS channel M15

VIIRS M15 Proxy (MODIS channel 31)

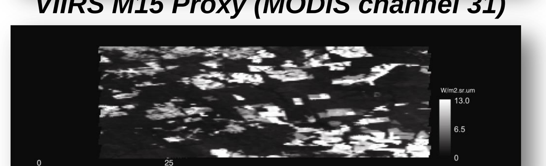

Simulated VIIRS M15

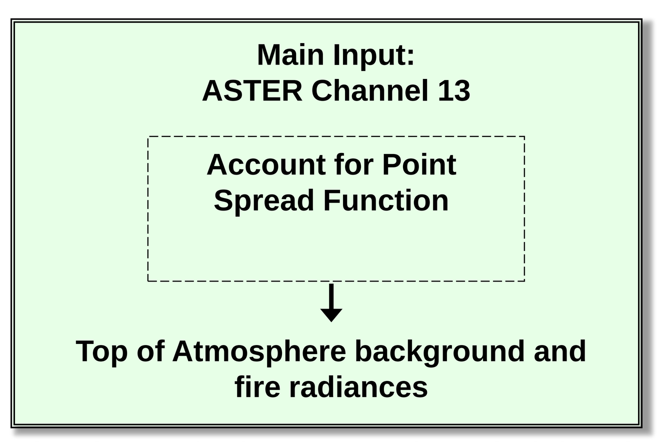

Flowchart of the VIIRS thermal infrared (channel M15) radiance calculation process

Middle Infrared Data

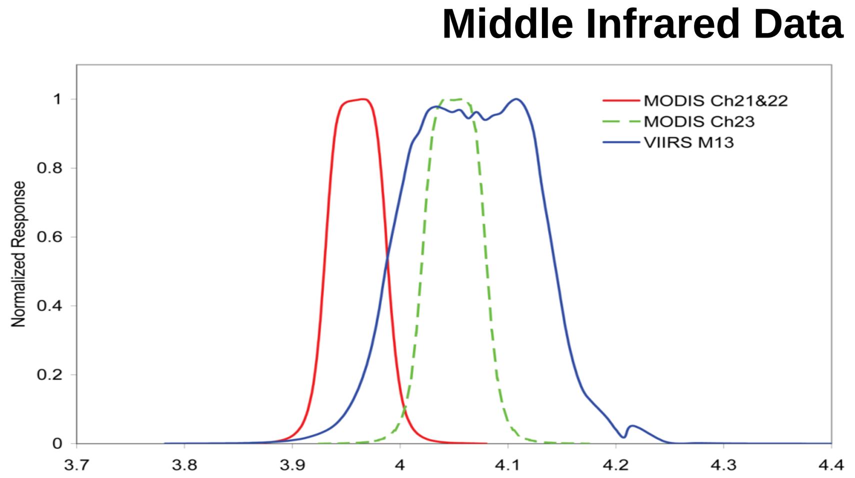

ASTER has no middle infrared bands. As an alternative, ASTER 90m surface kinetic temperature (AST_08) and 30m active fire mask data are used to generate 750m VIIRS M13 middle infrared channel.

Spectral response curves for MODIS channels 21-23, and VIIRS chanel M13

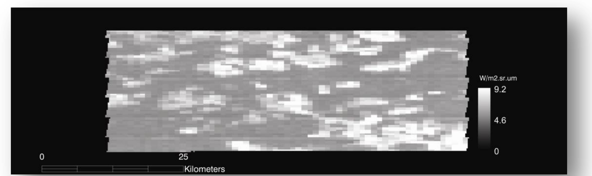

VIIRS M13 Proxy (MODIS Channel 21)

Simulated VIIRS M13

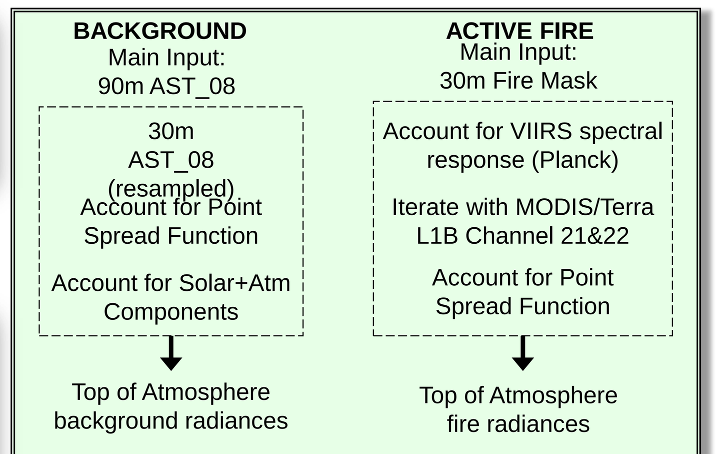

Flowchart of the VIIRS middle infrared (channel M13) radiance calculation process

EVALUATION OF SIMULATED VIIRS FIRE PIXEL RADIANCES

In the absence of independent reference datasets, the methodology for VIIRS fire pixel radiance simulation was tested by the accuracy to reproduce MODIS radiances. The working hypothesis was then to assume accurate sub-pixel fire characteristics to enable the simulation of radiances over the VIIRS pixel grid.

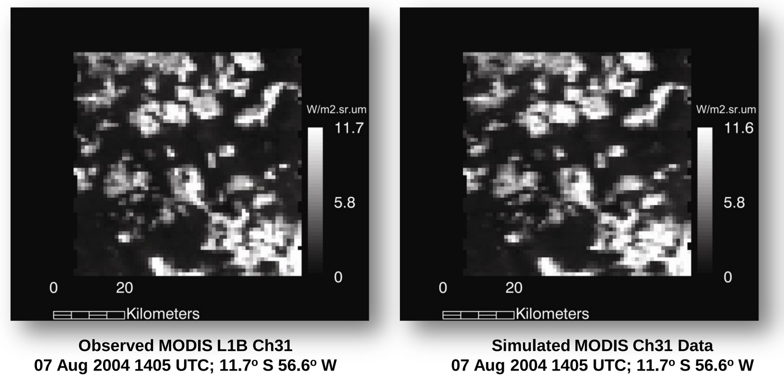

Observed and simulated scenes of LWIR MODIS radiances

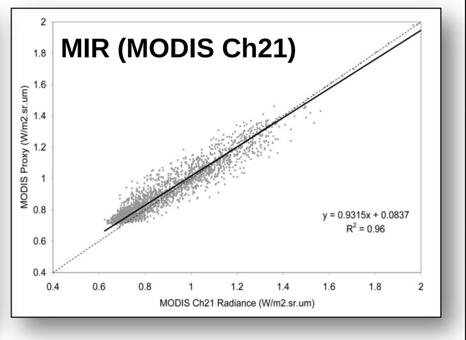

Simulated vs. observed LWIR MODIS radiances

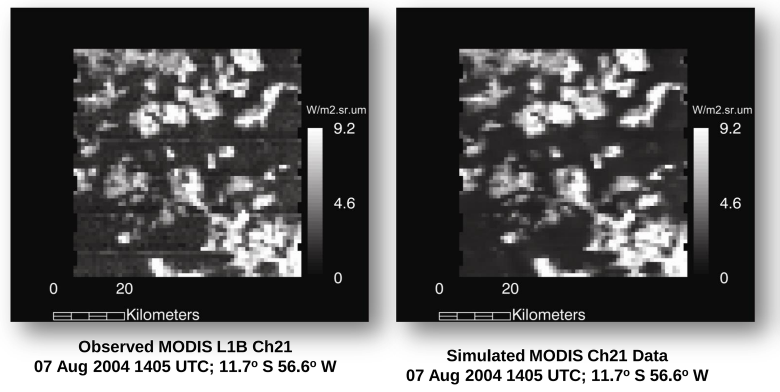

Observed and simulated scenes of MIR MODIS radiances

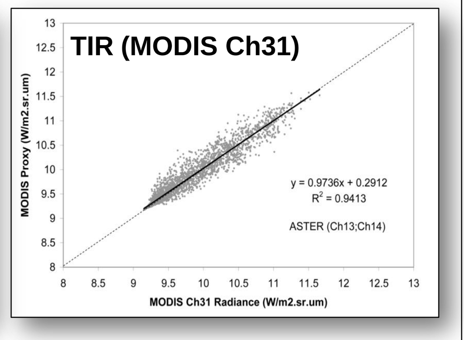

Simulated vs. observed MIR MODIS radiances

FIRE DETECTION FROM VIIRS

A: ALGORITHM REFINEMENTS BASED ON MODIS DEVELOPMENT

The current VIIRS Active Fires production code is based heavily on the Collection 4 MODIS fire detection algorithm. It is proposed that following enhancements, implemented in the Collection 6 MODIS algorithm, be incorporated in an improved VIIRS active fire detection algorithm:

- Adaptive assignment of potential fire thresholds to better capture small, cool fires and reduce false alarms occurring in hot, arid environments;
- A new rejection test to eliminate persistent false alarms caused by small clearings within Amazonian rainforest (see example below);
- Extended processing to water pixels to facilitate monitoring of offshore gas flaring (see example below);
- Improvements to the internal cloud mask to eliminate occasional misclassification of snow and desert as cloud.

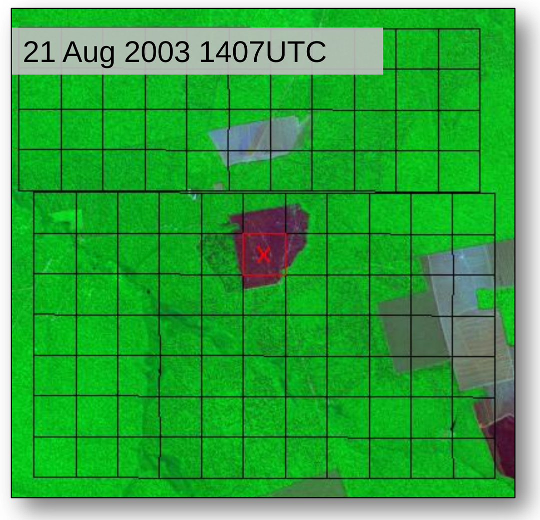

False alarm from Terra MODIS over a small-scale cleared area in the Amazon as detected by the MODIS Collection 5 algorithm

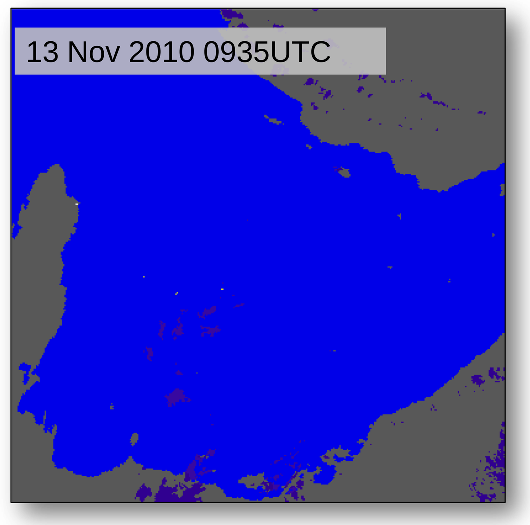

Aqua MODIS detections of off-shore gas flares in the Parsian Gulf as detected by the MODIS Collection 6 algorithm

B: VIIRS-SPECIFIC REFINEMENTS

The potential of a fire detection product from unaggregated pixel radiance data has been demonstrated (see an example below). Such a product would not only provide better geolocation and spatial detail of fire hot spots, but also detect smaller fires. However, the implementation of such a product involves major data preprocessing changes and therefore alternative approaches need to be thoroughly evaluated.

Additional potential VIIRS-specific refinements will exploit the higher resolution VIIRS imaging bands to reduce certain types of false alarms, and provide greater precision in the geolocation of active fires.

ASTER data (background RGB bands 8-3-1) acquired on Aug 07 2004; Left panel: 1km MODIS Terra coincident data; center panel: VIIRS aggregated proxy data (750x750m); right panel: VIIRS unaggregated proxy data (250x750m). Fire pixels are marked in red.

GLOBAL SIMULATIONS OF VIIRS FIRE PIXEL RADIANCES

Production of the fire mask requires MIR and LWIR observations but can tolerate saturation of either band provided that it occurs well above the maximum radiance that can be observed over the hottest and brightest clear land pixels. Production of Fire Radiative Power (FRP) requires unsaturated MIR observations. Retrievals of sub-pixel fire area and temperature and smoldering ratio require unsaturated LWIR radiances.

In the case of VIIRS, SWIIR band M13 is expected to produce unsaturated radiances for the vast majority of fires. However, the LWIR band M15 has low enough saturation levels to produce saturated radiances for a non-negligible percentage of fires.

A: DIRECT SIMULATION USING TERRA MODIS AND ASTER

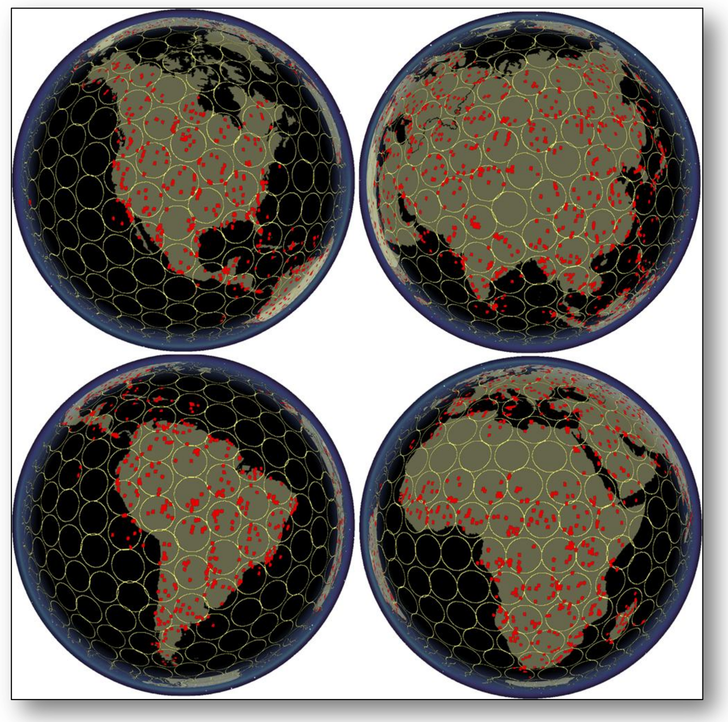

The cases analyzed are a subset of a dataset of ~3000 scenes from 2001-2006 used for the global validation of the standard MOD14 product using ASTER data mapped into Terra/MODIS pixel footprints as reference to determine sub-pixel fire characteristics.

Global distribution of ASTER scenes used for VIIRS fire pixel radiance simulation

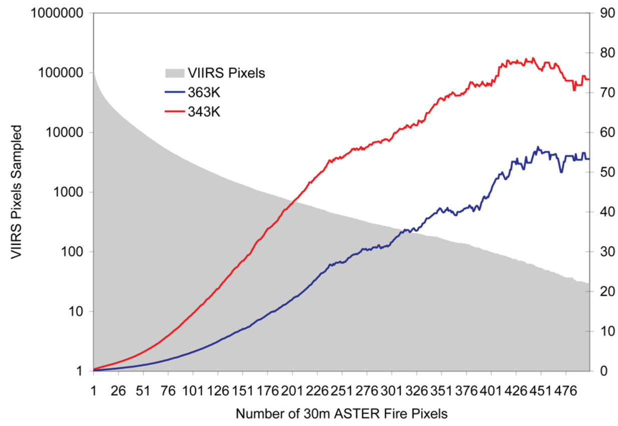

Percentage of aggregated VIIRS band M15 saturated pixels as a function of the number of ASTER 30m active fire pixels contained within the VIIRS pixel footprint. The two curves show the percentage of saturated M15 fire pixels assuming two distinct saturation temperatures.

The data are based on more than 110,000 simulated VIIRS pixels. Regional statistics of fire pixel saturation can depart significantly from the global mean value reaching levels as high as 75%.

B: STATISTICAL SIMULATION USING AQUA MODIS

An empirical relationship between MODIS and VIIRS radiances was derived using radiative transfer simulations. The approach assumes all of the fires within a 1-km MODIS reside within a single VIIRS unaggregated M15 pixel. For long fire fronts and/or large smoldering areas this assumption is usually not the case, and the approach will consistently overestimate the likelihood that an unaggregated VIIRS M15 pixels will saturate.

The results were partitioned into best-case (10[th] percentile), typical-case (50[th] percentile), and worst-case (90[th] percentile) scenarios for the empirical relationships.

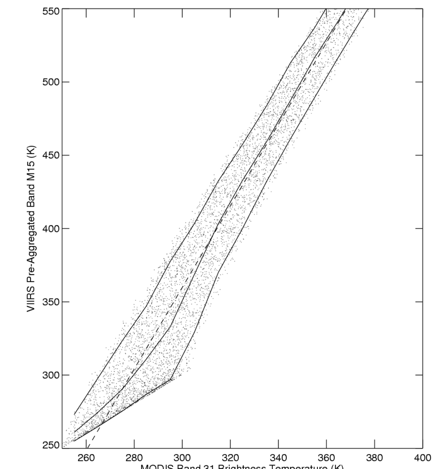

Simulated VIIRS M15 brightness temperature of a 259-m × 776-m unaggregated M15 pixel as a function of simulated MODIS band 31 brightness temperature of a 1-km MODIS pixel over a wide range of fire sizes and temperatures and surface and atmospheric conditions. Solid lines represent best-case (10[th] percentile), typical-case (50[th] percentile), and worst-case (90[th] percentile) empirical relationships used in new analysis.

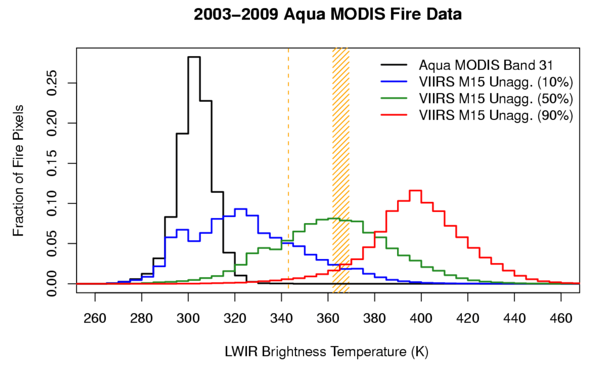

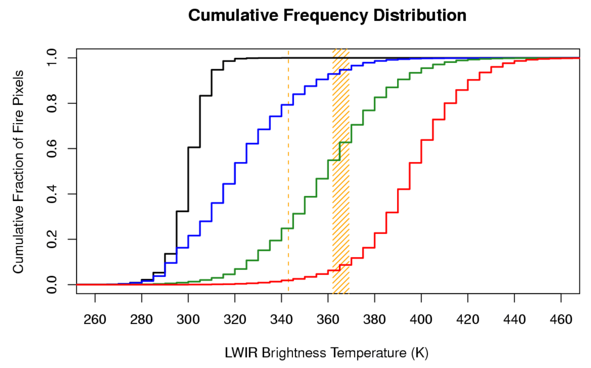

LWIR brightness-temperature frequency distributions for all Aqua MODIS fire pixels detected from 2003-2009 globally (black curve), with corresponding VIIRS M15 frequency distributions estimated using best-case (10[th] percentile), typical-case (50[th] percentile), and worst-case (90[th] percentile) empirical relationships derived from simulated MODIS and VIIRS fire scenes.

Orange vertical line is located at the 343 K VIIRS saturation specification, and vertical orange band indicates the range of measured saturation levels of the individual M15 detectors for the NPP VIIRS.

VIIRS ACTIVE FIRE PRODUCT VALIDATION

The transient nature of active fires requires near-coincident reference data at the pixel scale. Ground point measurements provide limited information over heterogeneous sites. Airborne sensors provide fine detail quality data although coverage is limited. Landsat-class sensors provide relatively good coverage but data quality tends to be limited for fire applications (e.g., pixel saturation)

A validation system for active fire algorithms was developed for 30m ASTER data and further adapted to Landsat TM and ETM+. ASTER is coincident with MODIS/Terra near nadir pixels (1km res). Landsat TM and ETM+ near coincident with MODIS/Terra off-nadir pixels (>18° scan angle; >1km res).

Probability of detection curves, omission and commission errors were quantified based on per pixel summary fire statistics using 30m reference data. Saturation problems and missing middle-infrared (MIR) band in Landsat-class data limits fire characterization assessment (e.g., Fire Radiative Power).

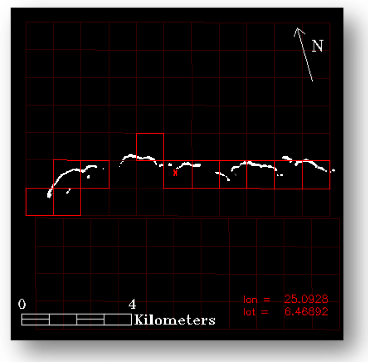

MODIS/ASTER 19 Jan 2006 0852UTC (near nadir)

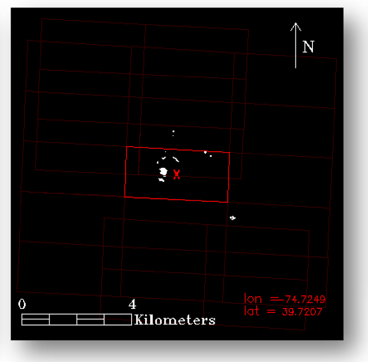

MODIS/TM 04 Aug 2007 1533UTC (52° scan angle)

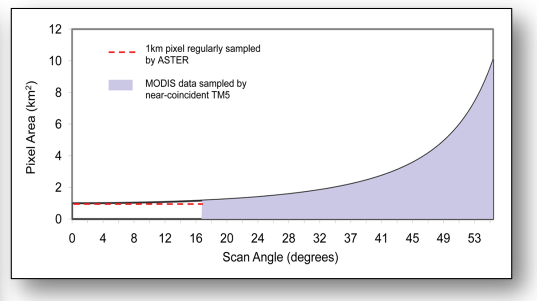

Angular coverage of MODIS pixels by simultaneous ASTER or Landsat-5 TM observations

Near-coincident fire detection is achievable between MODIS/Terra and ASTER and MODIS/Terra and Landsat TM across nearly all observation conditions.

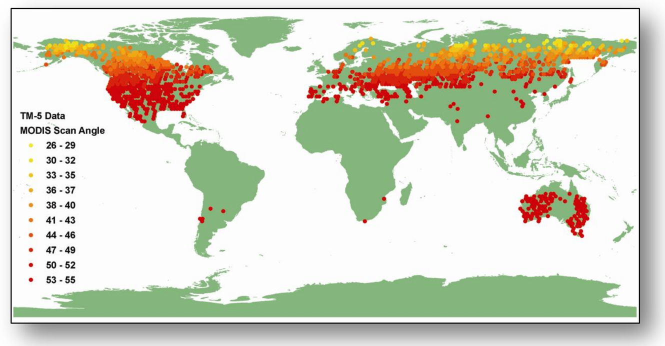

Global map of Landsat-5 TM scenes with fire observations, coincident with Terra MODIS

The basis of the VIIRS active fire validation protocol builds on protocols developed for MODIS active fire validation. The objective is to use fine resolution data sets as a proxy to investigate/validate fire detection algorithm performance, pixel saturation levels and data resampling scheme.

However, no fine resolution Landsat-class data is expected to fly near-coincidently with NPP/VIIRS. An alternative needs therefore to be developed based on refined data simulation. MODIS/Terra can be used as a laboratory to test data simulation methods and to verify quality of results. Supporting analyses using available airborne, spaceborne fine resolution reference active fire data constrain fire/background conditions to allow for applying realistic fire and background conditions in the data simulation.

NASA/AMES AMS Linescanner

Channel	Spectral Range
1	0.42 – 0.45 µm
2	0.45 – 0.52 µm
3	0.52 – 0.60 µm
4	0.60 – 0.62 µm
5	0.63 – 0.69 µm
6	0.69 – 0.75 µm
7	0.76 – 0.90 µm
8	0.91 – 1.05 µm
9	1.55 – 1.75 µm (high gain)
10	2.08 – 2.35 µm (high gain)
11	3.60 – 3.79 µm (high gain)
12	10.26 – 11.26 µm (high gain)
13	1.55 – 1.75 µm (low gain)
14	2.08 – 2.35 µm (low gain)
15	3.60 – 3.79 µm (low gain)
16	10.26 – 11.26 µm (low gain)

Landsat Class
VIIRS

USFS FireMapper Focal Plane Array

Channel	Spectral Range
1	0.60 – 0.70 µm
2	0.80 – 0.90 µm
3	1.58 ± 0.05 µm
4	3.9 ± 0.05 µm
5	8.30 – 8.80 µm
6	11.40 – 12.40 µm

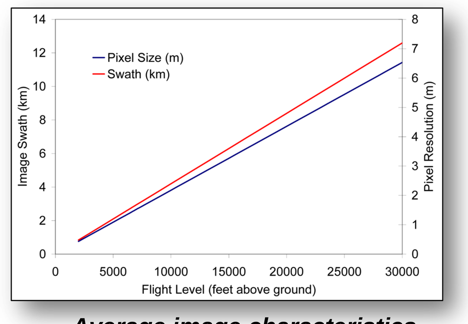

Average image characteristics

Poomacha Fire, San Diego County, California, 27 October 2008

As viewed at 10.5-µm wavelength in the thermal infrared by the NASA Autonomous Modular System (AMS) aboard the Ikana UAV (U.S. Forest Service image). The FireMapper color scheme has been applied.

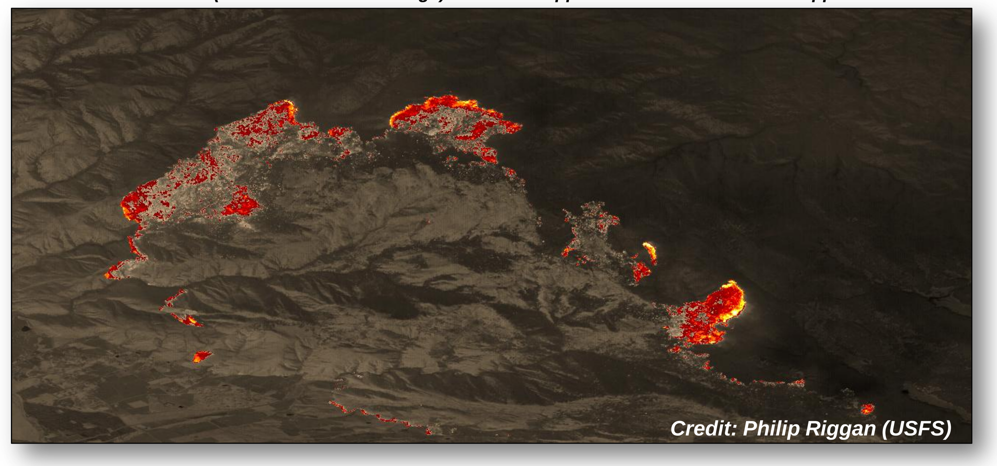

Esperanza Fire, Riverside County, California, 26 October 2006

As viewed at 14:12 PST by the FireMapper at 11.9-µm wavelength in the thermal infrared.